



5-Chloroanthranilic Acid Schiff Base: Crystal structure, DNA/BSA Interactions, Molecular Docking and Antioxidant Activity

5-Kloroantranilik Asit Schiff Bazı: Kristal Yapısı, DNA/BSA Etkileşimleri, Moleküler Bağlanma ve Antioksidan Aktivitesi

Duygu İnci Özbağcı[✉]

Department of Chemistry, Faculty of Arts and Sciences, Bursa Uludag University, Bursa, Turkey.

ABSTRACT

A novel 5CIAA-Schiff base (Schiff base derived from the condensation of 5-chloroanthranilic acid and 4-(dimethylamino)benzaldehyde) has been synthesized. The structure of the 5CIAA-Schiff base was clarified by CHN analysis, FTIR, electronic absorption spectroscopy, ESI-MS, and single-crystal X-ray diffraction methods. In biological activity studies, the interactions of the 5CIAA-Schiff base with calf thymus DNA (CT-DNA) were examined using fluorescence spectroscopy. The interactions of the 5CIAA-Schiff base with bovine serum albumin (BSA) were investigated using electronic absorption and fluorescence spectroscopy techniques, and the BSA quenching mechanism was found. The molecular docking simulation was analyzed to explore the interactions between the 5CIAA-Schiff base and biomolecules such as DNA and BSA using in silico techniques. Results confirmed that the 5CIAA-Schiff base was inserted into DNA via a minor groove and into BSA with subdomain IIA. The antioxidant activity of the 5CIAA-Schiff base was also investigated in comparison with the compounds used as standard.

Key Words

5-chloroanthranilic acid, Schiff base, DNA/BSA interactions, antioxidant activity.

Öz

Yeni bir 5CIAA-Schiff bazı (5-kloroantranilik asit ve 4-(dimetilamino)benzaldehit kondenzasyonundan türemiş) sentezlenmiştir. 5CIAA-Schiff bazının yapısı CHN analizi, FTIR, elektronik absorpsiyon spektroskopisi, ESI-MS ve X-ışını tek kristal kırınım yöntemleri ile aydınlatılmıştır. Biyolojik aktivite çalışmalarında, 5CIAA-Schiff bazının buzağı timüsü DNA'sı (CT-DNA) ile etkileşimleri floresans spektroskopisi kullanılarak incelenmiştir. 5CIAA-Schiff bazının sığır serum albümini (BSA) ile etkileşimleri elektronik absorpsiyon ve floresans spektroskopi teknikleri kullanılarak araştırılmış ve BSA sönümlenme mekanizması belirlenmiştir. 5CIAA-Schiff bazı ile DNA ve BSA gibi biyomoleküller arasındaki etkileşimleri in silico teknikleri kullanarak araştırmak için moleküler bağlanma çalışmaları gerçekleştirilmiştir. Sonuçlar, 5CIAA-Schiff bazının bir minör oluk aracılığıyla DNA ve alt subdomain IIA ile BSA ile etkileşime girdiğini doğrulamıştır. Ayrıca, 5CIAA-Schiff bazının antioksidan aktivitesi standart olarak kullanılan bileşiklerle karşılaştırmalı olarak araştırılmıştır.

Anahtar Kelimeler

5-kloroantranilik asit, Schiff bazı, DNA/BSA etkileşimleri, antioksidan aktivite.

Article History: May 7, 2024; Accepted: Aug 26, 2024; Available Online: Dec 11, 2024.

DOI: <https://doi.org/10.15671/hjbc.1495468>

Correspondence to: D.İ. Özbağcı, Department of Chemistry, Faculty of Arts and Sciences, Bursa Uludag University, Bursa, Turkey.

E-Mail: dyinginci@uludag.edu.tr

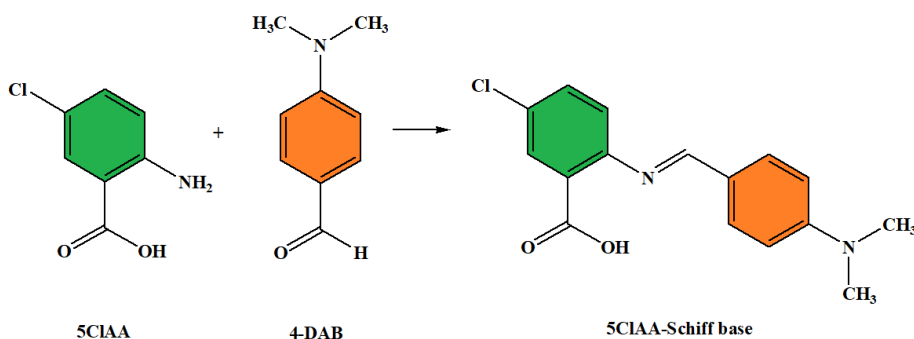
INTRODUCTION

Schiff bases are obtained by condensation reaction of primary amines under certain conditions by replacing the carbonyl groups in aldehydes or ketones with an imine or azomethine group [1]. Due to their easy synthesis and high yields, Schiff bases are among the most preferred compounds in scientific studies. Schiff bases could form complexes with almost all metal ions thanks to the imine nitrogen and the donor atoms in other functional groups such as phenoxyl oxygen atom, thiol sulfur atom, and carboxylate. Therefore, Schiff bases can easily form complexes thanks to the N, S, and O donor atoms in their structures. The type and number of these atoms have a great influence on the complex structure and diversity. Due to the unshared electron pair on the nitrogen atom, it is understood that Schiff bases also behave like Lewis bases. Because of this electron pair, they can be considered as σ donor ligands and can form stable complexes with coordinated covalent bonds with metal atoms. Developments in the field of bioinorganic chemistry and the understanding that Schiff base complexes can be used as models for biologically important species have increased interest in these complexes [2-4]. DNA, protein, and enzyme interactions have a very important place in biological studies related to the discovery of new compounds with drug potential.

Aromatic aldehydes have an efficient conjugation system, and thus, they are more stable than aliphatic ones [5]. 4-(dimethylamino) benzaldehyde is one of the aromatic aldehydes shown to have biological activity [6,7]. Recently, Al-Noor et al. reported that Schiff bases containing 4-(dimethylamino)benzaldehyde and 2-aminobenzoic acid have been synthesized and characterized by using techniques such as CHN elemental analyses, molar conductivity, magnetic moment, and

spectroscopic studies [8]. In addition, Schiff base containing 4-(dimethylamino)benzaldehyde and 2-aminobenzoic acid and its Mn(II) complex has been shown to have various bioactivities such as antimicrobial and antifungal activity reported by Ahmed and Aliyu. They found that the synthesized complex and Schiff base have the potential to be developed into novel antimicrobial and antifungal drugs [9]. Another feature that metal complexes of Schiff bases show is antioxidant activity; that is, they have a high capacity to scavenge free radicals [10,11]. Free radicals play a role as an important factor in the development of oxidative damage diseases. Therefore, there is a significant need for antioxidants as a defense against free radical attacks [12,13].

In light of this information, this study focuses on the synthesis, characterization, molecular docking, and elucidation of the biological activities of the new Schiff base, providing a new perspective for the development of complexes that prevent oxidative stress and may be drug candidates. Although similar compounds are found in the literature, we did not come across a study investigating the interaction with biomolecules, molecular binding studies and antioxidant capacity of the molecule we examined in this article. Our initial studies guiding the study were previously conducted and published by our group [14-17]. Our previous work encouraged us to synthesize a new 5ClAA-Schiff base (Scheme 1) and characterization. In the research of the biological activities of the 5ClAA-Schiff base, (i) interaction with CT-DNA using fluorescence spectroscopy (EB and Hoechst 33258 displacement assay); (ii) interaction with BSA using electronic absorption and fluorescence spectroscopies; (iii) antioxidant activity. Molecular docking studies were also conducted to observe the different weak and strong interactions with DNA and BSA. These studies provide insights into the binding pockets, amino acid residue, affinities, and type of interactions.



Scheme 1. Procedure for the synthesis of the 5ClAA-Schiff base.

MATERIALS and METHODS

The materials and methods, X-ray structure, investigation of CT-DNA/BSA interactions, antioxidant activity, and docking studies are presented in Supplementary Information.

Synthesis of the 5CIAA-Schiff base

1 mmol of 4-(dimethylamino)benzaldehyde was dissolved in 10 mL of methanol. 1 mmol of 5-chloroanthranilic acid solution dissolved in 10 mL of methanol was added slowly, and this mixture was stirred at room temperature for 4 hours. Dark orange crystals of 5CIAA-Schiff base suitable for single-crystal X-ray analysis were grown by slowly evaporating the resulting solutions at room temperature.

Yield was 79 %. Anal. calcd. for $C_{30}H_{27}Cl_3N_4O_6$ (645.90 g mol⁻¹) (%): C, 55.8; H, 4.2; N, 8.7. Found: C, 55.9; H, 3.9; N, 8.6. FTIR: 1601 ν (C=N), 1685 ν (C=O), 1477 ν (COO⁻) (Figure S1). UV-Vis (λ_{nm} , nm in DMSO): 250.4 (32687.1 M⁻¹ cm⁻¹), 351.5 (44147.1 M⁻¹ cm⁻¹) and 465.9 (2306.1 M⁻¹ cm⁻¹) (Figure S2). ESI-MS (m/z): 303.0921 for [5CIAA-Schiff base + H]⁺ (Figure S3).

RESULTS and DISCUSSION

Crystal Structure of 5CIAA-Schiff base

To obtain a better understanding of the molecular structure of the 5CIAA-Schiff base, its crystal structure was clarified via X-ray crystallography (Figure 1), and crystallographic data refinement is listed in Table 1. The crystal structure resulted as a supramolecular co-

Table 1. Crystallographic data and refinement parameters for the 5CIAA-Schiff base.

CCDC No	2343797
Empirical formula	$C_{30}H_{27}Cl_3N_4O_6$
Formula weight (g mol ⁻¹)	645.90
Temperature/K	298
Crystal system	monoclinic
Space group	$P2_1/n$
a/Å	7.140(2)
b/Å	13.948(4)
c/Å	29.243(8)
$\alpha/^\circ$	90
$\beta/^\circ$	94.344(7)
$\gamma/^\circ$	90
Volume/Å ³	2903.9(14)
Z	4
ρ_{calc}/cm^3	1.477
μ/mm^{-1}	0.368
F(000)	1336.0
Crystal size/mm ³	0.609 × 0.06 × 0.055
Radiation	MoK α ($\lambda = 0.71073$)
2 θ range for data collection/ $^\circ$	3.236 to 50.052
Index ranges	-8 ≤ h ≤ 8, -16 ≤ k ≤ 16, -34 ≤ l ≤ 34
Reflections collected	26463
Independent reflections	5138 [$R_{int} = 0.0745$, $R_{sigma} = 0.0645$]
Data/restraints/parameters	5138/0/395
Goodness-of-fit on F^2	1.027
Final R indexes [$I \geq 2\sigma(I)$]	$R_1 = 0.0489$, $wR_2 = 0.1003$
Final R indexes [all data]	$R_1 = 0.0945$, $wR_2 = 0.1179$
Largest diff. peak/hole / e Å ⁻³	0.36/-0.27

crystal of 5-chloroanthranilic acid with the Schiff base-derived compound ((E)-5-chloro-2-((4-(dimethylamino)benzylidene)amino)benzoic acid) bearing the azomethine (–C=N–) functional group in a 2 to 1 ratio. (E)-5-chloro-2-((4-(dimethylamino)benzylidene) amino)benzoic acid shows an almost entirely planar molecular conformation with a negligible interplanar twist. As given in the hydrogen bonding analysis (Table 2), there are three different intramolecular hydrogen bonding interactions (N3—H3A···O2, N4—H4A···O3, O6—H6···N2) in the typical crystal structure. The crystal structure is stabilized mainly by intermolecular N—H···O (N3—H3A···O3, N3—H3B···O1), O—H···O (O4—H4···O5, O2—H2···O6) and weak C—H···O (C6—H6A···O1 and C8—H8···O3) interactions. Also, it should be noted that one C—H··· π interaction (C15—H15··· π , $d(\text{H}\cdots\pi) = 2.87 \text{ \AA}$) exists between the 5CIAA-Schiff base molecule and 5-chloroanthranilic acid.

DNA binding activities

Fluorescence spectroscopy studies were investigated by two methods, EB displacement and Hoechst 33258. Displacement studies were performed with EB. The electronic absorption spectrum of EB showed an absorbance maximum at 480 nm. Therefore, excitation was performed at 480 nm for EB+CT-DNA and EB+CT-DNA+5CIAA-Schiff base solutions, and fluorescence spectra were taken in the wavelength range of 500-700 nm. As the 5CIAA-Schiff base concentration was increased, decreases in the fluorescence intensity of EB+DNA solution was observed (Figure 2). The K_{sv} , expressing the fluorescence quenching ability of the 5CIAA-Schiff base was found using the equation $I_0/I = 1 + K_{sv} \cdot [5\text{CIAA-Schiff base}]$. The K_{sv} was calculated from the slope of the line obtained by plotting I_0/I values against $[5\text{CIAA-Schiff base}]$ values [18].

Schiff base] values [18]. The calculated $\log K_{sv}$ value was found to be 3.66. After calculating K_{sv} , the value expressing the fluorescence quenching abilities of the 5CIAA-Schiff base, K_{app} value was calculated by utilizing the changes in fluorescence intensities in response to increasing the 5CIAA-Schiff base concentration, where the 5CIAA-Schiff base reduced the fluorescence intensity of EB+CT-DNA solution to 50%. The K_{app} value of the 5CIAA-Schiff base was found using the equation $K_{app} \cdot [5\text{CIAA-Schiff base}] = K_{EB} \cdot [\text{EB}]$ [19], and the calculated $\log K_{app}$ value was found to be 5.40.

To find the binding mode of the 5CIAA-Schiff base to CT-DNA, displacement studies were performed using Hoechst 33258, which is known to bind to CT-DNA through minor grooves. Hoechst 33258+CT-DNA and Hoechst 33258+CT-DNA+5CIAA-Schiff base solutions were excited at 351 nm, and fluorescence spectra were taken in the wavelength range 400-650 nm. As the 5CIAA-Schiff base concentration increased, a decline in the fluorescence intensity of the Hoechst 33258+DNA+5CIAA-Schiff base solution was observed (Figure 2). The K_{sv} , expressing the fluorescence quenching ability of the 5CIAA-Schiff base was found using the equation $I_0/I = 1 + K_{sv} \cdot [5\text{CIAA-Schiff base}]$. The K_{sv} was calculated from the slope of the line obtained by plotting I_0/I values against $[5\text{CIAA-Schiff base}]$ values [18]. The calculated $\log K_{sv}$ value was found to be 4.37. The experimental results obtained were evaluated with the classical Stern-Volmer equation [18, 20] to define the interaction strength of the 5CIAA-Schiff base with CT-DNA. When the $\log K_{sv}$ value obtained by adding the 5CIAA-Schiff base to EB+CT-DNA solution was compared with the $\log K_{sv}$ value obtained by adding the 5CIAA-Schiff base to Hoechst 33258+CT-DNA solution, it was observed

Table 1. Crystallographic data and refinement parameters for the 5CIAA-Schiff base.

D—H···A	Symmetry codes	D—H	H···A	D···A	D—H···A
N3—H3A···O3	x, y, z	0.86	2.602	3.270(4)	135.1
N3—H3B···O1	-1+x, y, z	0.86	2.201	2.929(4)	142.0
N3—H3A···O2	x, y, z	0.86	2.179	2.664(4)	115.4
N4—H4A···O3	x, y, z	0.86	2.050	2.700(4)	131.5
O4—H4···O5	x, y, z	0.82	1.771	2.577(3)	167.5
O2—H2···O6	x, y, z	0.82	1.775	2.578(3)	165.5
O6—H6···N2	x, y, z	0.82	1.803	2.561(3)	153.2
C6—H6A···O1	x, y, z	0.93	2.633	3.297(4)	128.8
C8—H8···O3	1-x, 1-y, 1-z	0.93	2.532	3.287(4)	138.6

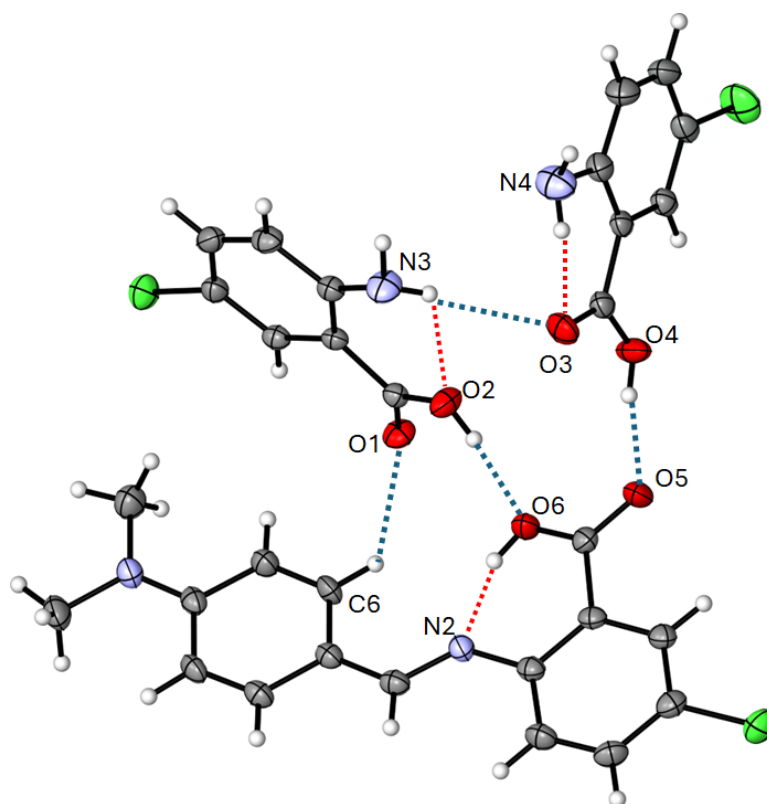


Figure 1. Crystal structure of the 5CIAA-Schiff base with displacement ellipsoids (30% probability level) showing the intra (red dotted lines) and intermolecular (blue dotted lines) hydrogen bonding interactions.

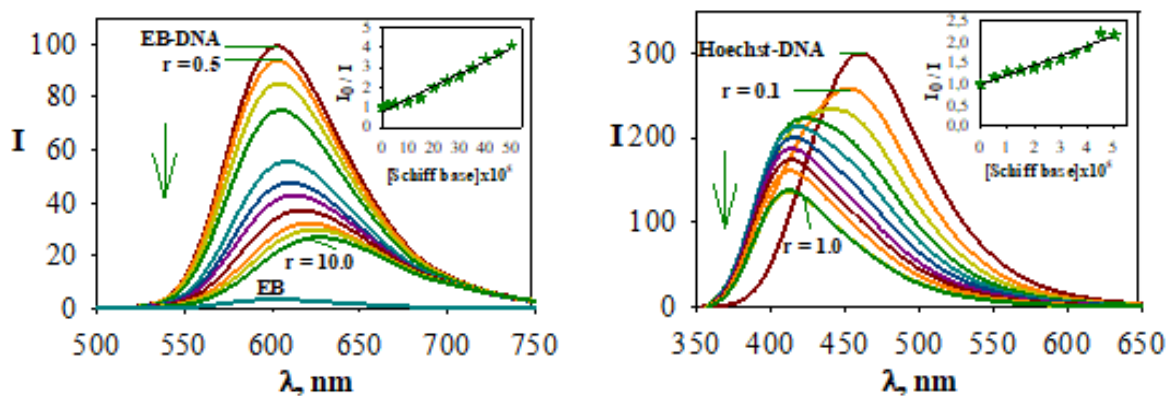


Figure 2. Effect of addition of the 5CIAA-Schiff base on the emission intensity of the CT-DNA bound EB and Hoechst 33342 at different concentrations.

that the $\log K_{sv}$ value of the 5CIAA-Schiff base were higher in Hoechst 33258+CT-DNA solution, indicating that the 5CIAA-Schiff base may interact through the minor groove in the CT-DNA structure.

Investigation of 5CIAA-Schiff base+BSA Interactions

The interactions of the 5CIAA-Schiff base with BSA were researched using fluorescence (fluorescence resonance energy transfer (FRET), synchronized fluorescence, three-(3D) two-(2D) dimensional fluorescence), and electronic absorption spectroscopy techniques.

Figure 3a indicates the electronic absorption spectra of BSA alone and the 5CIAA-Schiff base interaction with BSA. When the spectra of BSA alone and the 5CIAA-Schiff base+BSA were analyzed, an increase or decrease in absorbance and wavelength shifts were observed. From the electronic absorption spectroscopy results, it was interpreted that the quenching mechanism of the 5CIAA-Schiff base was static quenching.

As the 5CIAA-Schiff base concentration was increased, decreases in the fluorescence intensity of BSA were observed (Figure 3b). The Stern-Volmer constant, K_{sv} , and the biomolecular quenching rate constant, K_q , which express the fluo-

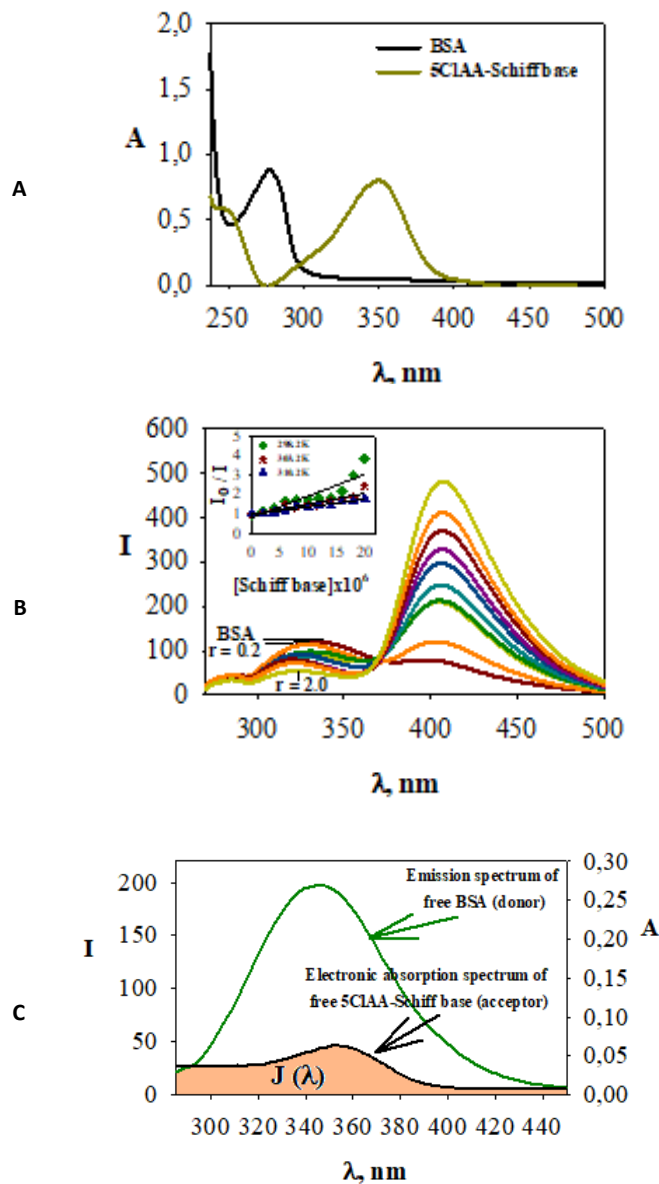


Figure 3. A. Electronic absorption spectra of 5CIAA-Schiff base upon addition of BSA, B. Effect of 5CIAA-Schiff base on the fluorescence spectra of BSA, C. The emission spectrum of BSA and electronic absorption spectrum of 5CIAA-Schiff base. A shaded region represents the overlapping area of both spectra.

rescence quenching abilities of the 5CIAA-Schiff base were determined. The K_{sv} was calculated from the slope of the line obtained by plotting I_0/I values against [5CIAA-Schiff base] values, and the biomolecular quenching rate constant, K_q , was calculated from the same equation [18]. The calculated $\log K_{sv}$ values were found to be 4.93 (25°C), 4.70 (30°C), 4.52 (37°C). The curves obtained using the Stern-Volmer equation for the 5CIAA-Schiff base were found to be linear and the slope decreased with increasing temperature. This suggested that the fluorescence quenching mechanism of the 5CIAA-Schiff base might be static. The calculated K_q values were found to be 12.93 (25°C), 12.70 (30°C), 12.52 (37°C). In addition, the biomolecular quenching rate constant, K_q , values were higher than the maximum diffusion collision quenching rate constant ($2.0 \times 10^{10} \text{ M}^{-1} \text{ s}^{-1}$), showing again that the quenching mechanism of the 5CIAA-Schiff base may be static [21]. The finding of static quenching as the fluorescence quenching mechanism for the 5CIAA-Schiff base agreed with the results obtained using electronic absorption spectroscopy. The modified Stern-Volmer binding constant, K_s , expresses the fluorescence quenching abilities of the 5CIAA-Schiff base. The $\log K_s$ values calculated for the 5CIAA-Schiff base were found to be 4.92 (25°C), 4.70 (30°C), 4.26 (37°C). The fluorescence intensity data measured while investigating the interactions of the 5CIAA-Schiff base with BSA could be used to find the binding constant (K_A) and the number of binding sites (n). The $\log K_A$ and n values were found to be 5.30 and $n = 1.08$ (25°C); 4.67 and $n = 0.99$ (30°C); 4.45 and $n = 0.98$ (37°C). The n values were approximately close to 1, suggesting that the 5CIAA-Schiff base interacted through a binding site of BSA. The thermodynamic parameters for the 5CIAA-Schiff base were calculated using the Van't Hoff equations. The calculated thermodynamic parameter values of the 5CIAA-Schiff base were found to be $\Delta H = -121.39$ and $\Delta S = -308.47$, $\Delta G = -29.42$ (25°C); -27.88 (30°C); -25.72 (37°C). The free energy change

values, ΔG , calculated from the data obtained as a result of the interaction of the 5CIAA-Schiff base with BSA were negative. This result indicated that the 5CIAA-Schiff base interacted spontaneously with BSA. The negative enthalpy and entropy values ($\Delta H < 0$ and $\Delta S < 0$) for the 5CIAA-Schiff base indicate that hydrogen bonding or van der Waals forces are active in their interaction with BSA. For Förster resonance energy transfer studies of the 5CIAA-Schiff base, solutions containing BSA and BSA+the 5CIAA-Schiff base were prepared ([BSA]=[5CIAA-Schiff base]=1 μM). Figure 3c shows the overlap between the emission spectra of BSA and the electronic absorption spectra of the 5CIAA-Schiff base. The calculated E and r values of the 5CIAA-Schiff base were found to be 44.39 % and 0.79 nm, respectively. The r value of the 5CIAA-Schiff base was smaller than 8 nm, indicating that radiation-free energy transfer between BSA and the 5CIAA-Schiff base occurred. This also indicated static quenching between BSA and the 5CIAA-Schiff base [22]. The binding site of the 5CIAA-Schiff base interacting with BSA and the distance between them cannot be determined precisely. However, reasonable interpretations can be made about the binding position and distance. The low r values indicated that the distance between BSA and the 5CIAA-Schiff base was close [23]. For synchronized fluorescence studies of the 5CIAA-Schiff base, BSA and BSA+the 5CIAA-Schiff base solutions were excited at 280 nm, and fluorescence spectra were taken with a wavelength difference of 15 nm and 60 nm. As the concentration of the 5CIAA-Schiff base increased, decreases in the fluorescence intensity of BSA were observed, and were plotted as values % (Figure 4).

When the fluorescence intensity values % obtained from the synchronized fluorescence spectra of the 5CIAA-Schiff base at 15 nm and 60 nm wavelength difference were analyzed, it was found that when the

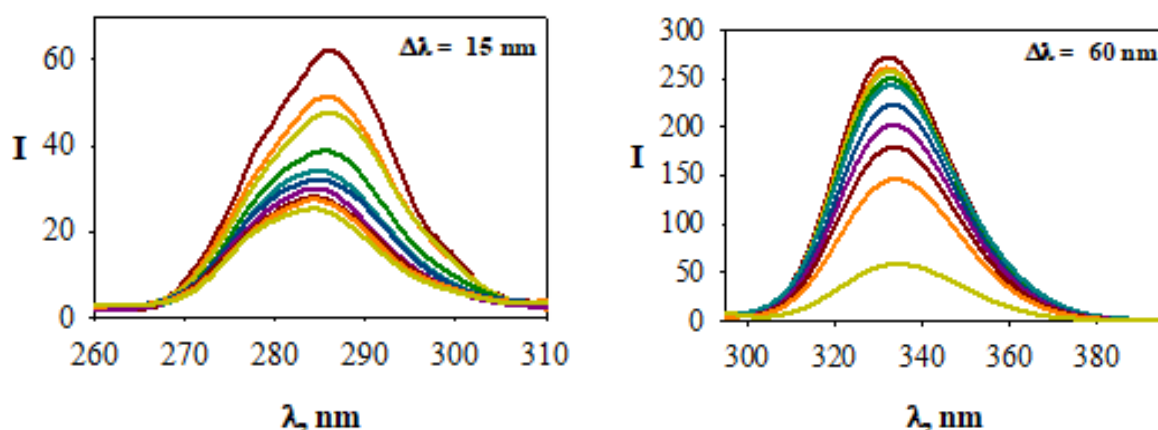


Figure 4. Synchronous fluorescence quenching of BSA in the presence of 5CIAA-Schiff base at $\Delta\lambda = 15 \text{ nm}$ and $\Delta\lambda = 60 \text{ nm}$.

wavelength difference was 15 nm, the emission intensity change was observed around 285 nm. When the wavelength difference was 60 nm, the emission intensity change was observed around 335 nm. The % fluorescence intensity values of tyrosine residues obtained from the synchronized fluorescence spectra of the 5CIAA-Schiff base at 15 nm wavelength difference were found to decrease (59.15 %). A decrease in the % fluorescence intensity values of tryptophan residues obtained from the synchronized fluorescence spectra of the 5CIAA-Schiff base at 60 nm wavelength difference was also observed (78.41 %). These results clearly showed that the 5CIAA-Schiff base altered the conformation of BSA, causing changes in the microenvironments in the region of tryptophan and tyrosine residues. In experimental studies using two-(2D) and three-(3D) dimensional fluorescence spectroscopy of the 5CIAA-Schiff base, solutions containing BSA and BSA+the 5CIAA-Schiff base were prepared ($[BSA]=1 \mu M$, $[5CIAA-Schiff \text{ base}]=1 \mu M$). The emission spectra of BSA alone and BSA+the 5CIAA-Schiff base solutions were taken in the

wavelength range 220-350 nm with excitation every 10 nm, and emission spectra were taken in the wavelength range 220-700 nm. It was observed that the fluorescence intensities reached the highest value when BSA alone and BSA+the 5CIAA-Schiff base solutions were excited at wavelengths of 280-290 nm, while the fluorescence intensities were lower when excited at other wavelengths. Figure 5 displays the spectral behavior of tyrosine and tryptophan residues with emission fluorescence intensity depending on the polarity of their microenvironment in the structure of BSA. The fluorescence intensities of BSA+the 5CIAA-Schiff base solutions were found to be lower than those of BSA alone. This indicates that the 5CIAA-Schiff base changes the microenvironment of tryptophan and tyrosine residues in the structure of BSA.

Molecular docking analysis

Molecular docking simulations were performed to better understand the interactions between the 5CIAA-Schiff base and DNA (BSA). The molecular docking

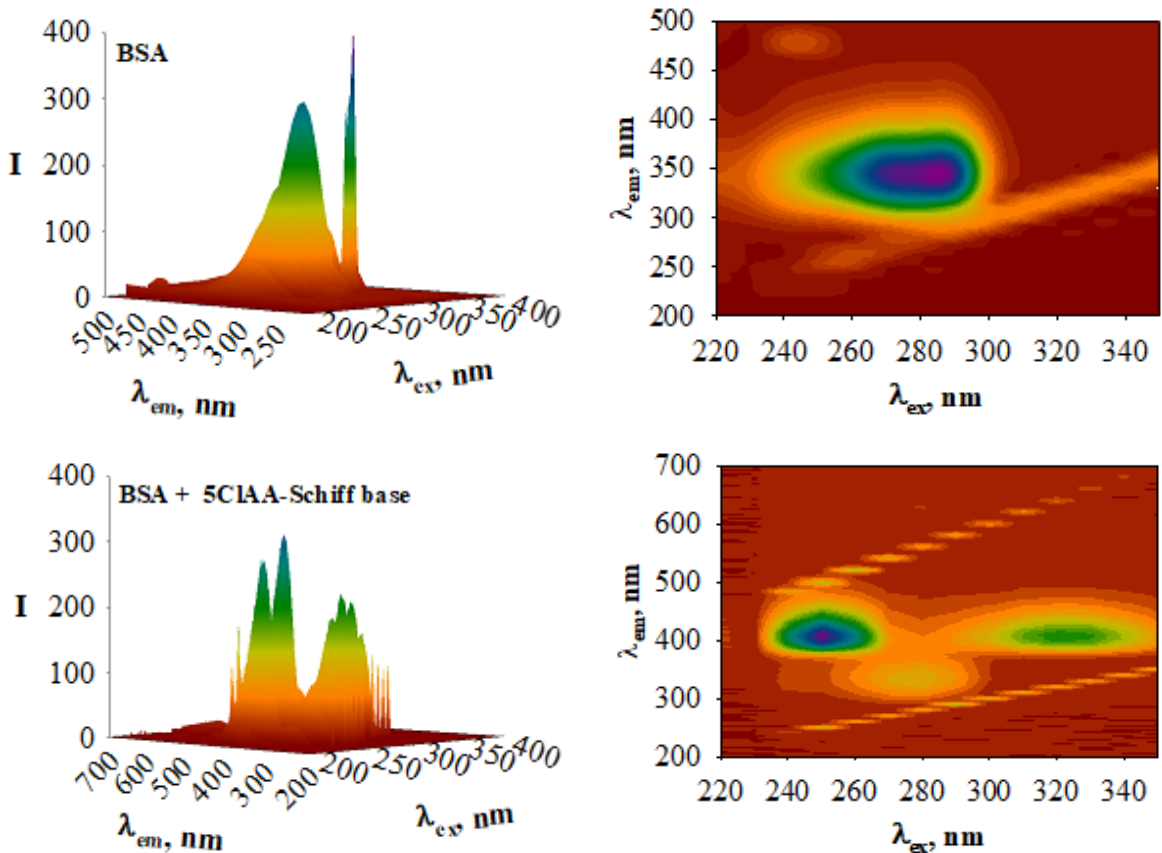


Figure 5. Three-dimensional and contour plot of the fluorescence spectra of BSA, BSA+5CIAA-Schiff base.

analysis results using the binding energies and involving residues are given in Table 3 and illustrated in Figures 6 and 7. The best-docked pose with 1BNA was demonstrated to bind to a minor groove of DNA with a binding energy of -8.11 kcal/mol (Figure 6) [24]. The DNA was efficiently bonded with the 5CIAA-Schiff base thoroughly with three strong conventional hydrogen bonds, of which DA17, DT8, and DC9. The bond lengths were $d = 2.62$ Å, 2.81 Å, and 2.96 Å, respectively. The 5CIAA-Schiff base interacted also several van der Waals interactions with other residues. Many anti-cancer agents have been identified to interact with the grooves of the DNA double helix, disrupting its function and impeding crucial cellular processes such as replication and transcription, consequently altering cell division [25].

A molecular docking simulation was performed to gain knowledge and insight into BSA with the 5CIAA-Schiff base. BSA contains two TRP residues responsible for tryptophan quenching experiments (TRP134 and

TRP213) [26]. TRP134 is located in domain I, which is a hydrophilic environment and on the surface of the BSA, while TRP213 is in domain II, which is a hydrophobic pocket (Figure 7) [27]. The docking result indicated that the 5CIAA-Schiff base interacted near TRP134 in domain I with π -alkyl interaction between the chlorine group and benzene ring of the TRP134 residue (5.37 Å). The binding energy was calculated as -7.97 kcal/mol. There are two alkyl interactions between the benzene ring of the 5CIAA-Schiff base and the carbon chain from the LYS132 and the VAL40 residues and two other alkyl interactions between the chlorine atom of the 5CIAA-Schiff base and the carbon chain from the LEU24 and LYS20 residues. Previous studies have identified this region as a binding site for BSA [28,29].

Antioxidant Activities of the 5CIAA-Schiff base

EC_{50} values of the antioxidant activities obtained for the 5CIAA-Schiff base and standard antioxidants were given in Table 4. The antioxidant activities of the 5CIAA-Schiff

Table 3. Docking results of the 5CIAA-Schiff base with DNA (PDB ID: 1BNA) and BSA (PDB ID: 4F5S).

Target	Docked score	D—H	H...A
(kcal/mol)	Number of hydrogen bonds	Interacting residues	2.602
DNA	-8.11	DA B: 17, DT A: 8, DC A: 9	DA B:18, DT B:19, DG A:10, DG B:16, DC A:11
BSA	-7.97	-	TRP134, LYS20, LEU24, VAL40, LYS132

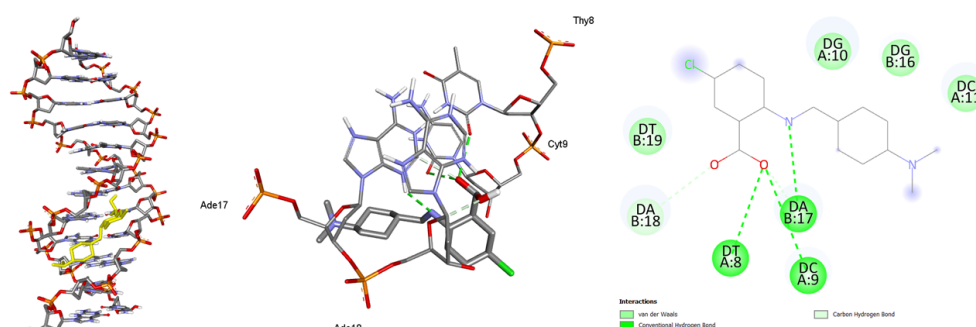


Figure 6. 3D docking structure, 2D and ligand interactions of the 5CIAA-Schiff base with active sites of B-DNA dodecamer (PDB ID: 1BNA).

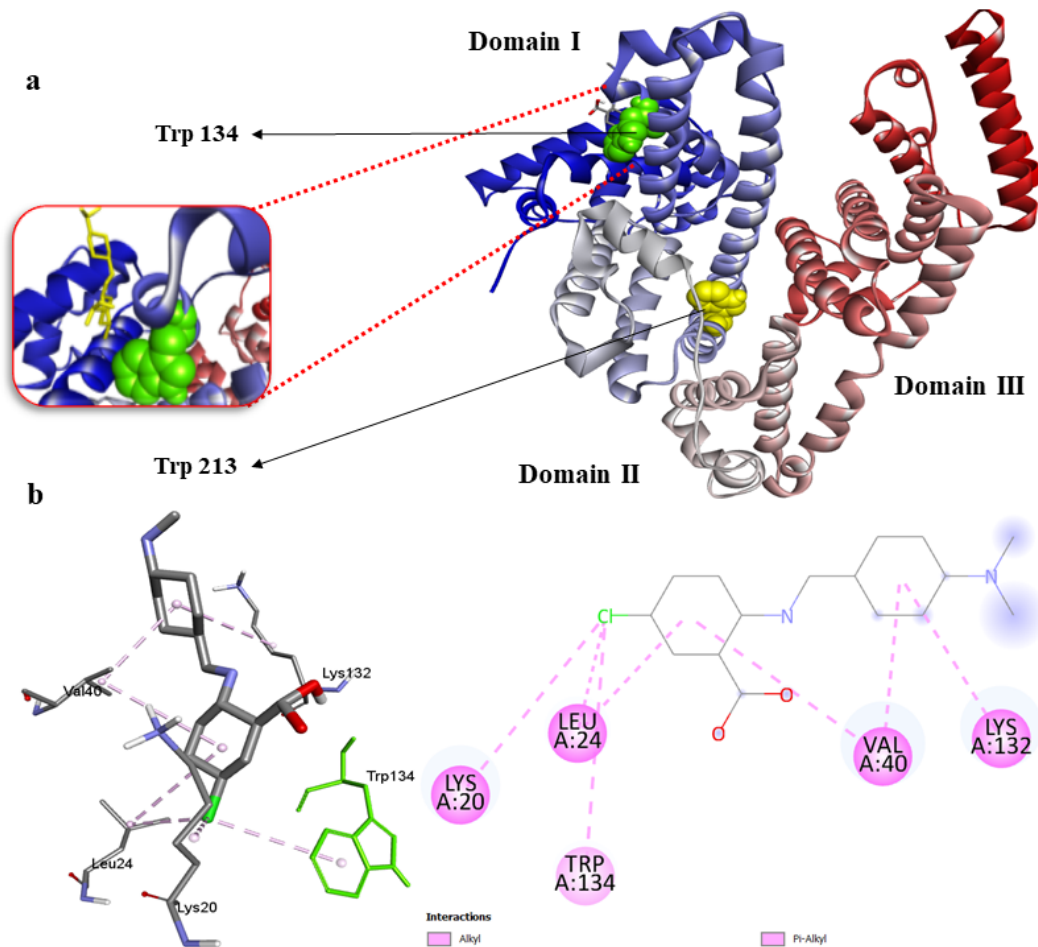


Figure 7. 3D docking structure (a), and ligand interactions, and 2D diagram (b) of the 5CIAA-Schiff base with active sites of BSA (PDB ID: 4F5S). The domain regions are delineated as follows: domain I (residues 1–195), domain II (residues 196–383), and domain III (residues 384–583).

base were calculated using the equation described in the “Antioxidant Activity” section in the supplementary material. According to the results obtained from the DPPH radical scavenging activities of the 5CIAA-Schiff base, compared to ascorbic acid (Asc), Trolox, and BHT used as standard, its activity was found to be low. But, compared to β -carotene, the 5CIAA-Schiff base was

found to have higher DPPH radical scavenging activity [30].

In conclusion, a novel 5CIAA-Schiff base (derived from the condensation of 5-chloroanthranilic acid and 4-(*dimethylamino*)benzaldehyde) was synthesized and structurally characterized. The CT-DNA binding studies of the

Table 4. The radical scavenging activities of the 5CIAA-Schiff base.

Compounds	EC ₅₀ (μM)	
	DPPH	Ref
5CIAA-Schiff base	49.9 ± 0.05	♣
Asc	25.6	[15]
Trolox	7.73	[15]
BHT	15.04	[15]
β -carotene	415.3	[30]

♣: In this study

5CIAA-Schiff base show that the 5CIAA-Schiff base interacts with CT-DNA via minor groove binding. The 5CIAA-Schiff base revealed a static mechanism in interaction with BSA. The other biophysical experiments such as synchronous fluorescence, 3D and 2D fluorescence, and FRET calculation provide strong evidence for interaction and conformational change of BSA with the 5CIAA-Schiff base. Furthermore, thermodynamic parameters indicated that the hydrogen bonding and van der Waals forces for the 5CIAA-Schiff base were the main forces driving the interaction with BSA. The 5CIAA-Schiff base demonstrated a strong radical scavenging activity when compared to standard antioxidant β -carotene. The docking studies revealed that the 5CIAA-Schiff base exhibited minor groove binding to the DNA and interacted in the vicinity of TRP134 of BSA in domain I. These interactions consisted of conventional hydrogen bonds and van der Waals interactions through B-DNA, while alkyl and π -alkyl interactions were observed with BSA.

Acknowledgments The author would like to thank Prof. Dr. Rahmiye Aydın for allowing me to use the facilities at the Inorganic Chemistry Laboratory to conduct in this study. The author also would like to acknowledge Prof. Dr. Yunus Zorlu for the discussion about the single-crystal X-ray diffraction data analysis and Assist. Prof. Dr. Sevinç İlkar Erdağlı for the discussion about the molecular docking data analysis.

References

- Z. Hussain, M. Khalaf, H. Adil, D. Zageer, F. Hassan, S. Mohammed, E. Yousif, Metal complexes of Schiff's bases containing sulfonamides nucleus: A review, *Res. J. Pharm. Biol. Chem. Sci.*, 7(2016) 1008-1025.
- S. Zehra, T. Roisnel, F. Arjmand, Enantiomeric amino acid Schiff base copper(II) complexes as a new class of RNA-targeted metallo-intercalators: single X-ray crystal structural details, comparative *in vitro* DNA/RNA binding profile, cleavage, and cytotoxicity, *ACS Omega* 4 (2019) 7691-7705.
- T. Hermann, Strategies for the design of drugs targeting RNA and RNA-protein complexes, *Angew. Chem. Int. Ed. Engl.*, 39 (2000) 1890-1905.
- K.A. Meadows, F. Liu, J. Sou, B.P. Hudson, D.R. McMillin, Spectroscopic and photophysical studies of the binding interactions between copper phenanthroline complexes and RNA, *Inorg. Chem.*, 32 (1993) 2919-2923.
- M. Asif, An overview on synthesis and medicinal chemistry potentials of biologically active antimicrobial Schiff's bases and its complexes: a review, *Mor. J. Chem.*, 3(3) (2015) 627-652.
- L. Kafi-Ahmadi, A.P. Marjani, M. Pakdaman-Azari, S. Afr, Synthesis, characterization and antibacterial properties of N,N'-Bis(4-dimethylaminobenzylidene)benzene-1,3-diamine as new Schiff Base ligand and its binuclear Zn(II), Cd(II) complexes. *J. Chem. Eng.*, (71) (2018) 155-159.
- S. S. Hassan, E. A. Bedir, A. E.-R. M. Hamza, A. M. Ahmed, N. M. Ibrahim, M. S. Abd El-Ghany, N. N. Khattab, B. M. Emeira, M. M. Salama, E. F. Mohamed, D. B. Fayed, The dual therapeutic effect of metformin nuclei-based drugs modified with one of Tulbaghia violacea extract compounds, *Appl. Organomet. Chem.* 36(9) (2022) e6804.
- T.H. Al-Noor, N.S. Al-barki, A.A. Maihub, M.M. El-ajaily, Synthesis and Spectroscopic Characterization of some Mixed Schiff Base Complexes, *International Journal of Science and Research (IJSR)*, 6(3) (2017) 2421-2426.
- A.A. Ahmed, H.N. Aliyu, Synthesis, Structural Characterization and Antimicrobial Potency of Anthranilic Acid Based Mn(II) Schiff Base Complex, *Chemistry Research Journal*, 4(5) (2019) 54-61.
- Y. Zhang, B. Zou, Z. Chen, Y. Pan, H. Wang, H. Liang and X. Yi, Synthesis and antioxidant activities of novel 4-Schiff base-7-benzoyloxycoumarin derivatives, *Bioorg. Med. Chem. Lett.*, (21) (2011) 6811-6815.
- W.A. Zoubi, A.A.S. Al-Hamdani, M. Kaseem, Synthesis and antioxidant activities of Schiff bases and their complexes: a review, *Appl. Organometal. Chem.*, 30 (2016) 810-817.
- K.J. Barnham, C.L. Masters, A.I. Bush, Neurodegenerative diseases and oxidative stress, *Nat. Rev. Drug Discov.*, 3(3) (2004) 205-214.
- B. Uttara, A.V. Singh, P. Zamboni, R.T. Mahajan, Oxidative stress and neurodegenerative diseases: a review of upstream and downstream antioxidant therapeutic options, *Curr. Neuropharm.*, 7(1) (2009) 65-74.
- D. Inci, R. Aydın, Y. Zorlu, NOO-type tridentate Schiff base ligand and its one-dimensional Cu(II) coordination polymer: synthesis, crystal structure, biomacromolecular interactions and radical scavenging activities, *Inorg. Chim. Acta* 514 (2021) 119994.
- D. Inci, A new ternary Cu (II) complex with 4,7-dimethyl-1,10-phenanthroline and NOO-type tridentate Schiff base ligand: synthesis, crystal structure, biomacromolecular interactions, and radical scavenging activities, *Appl. Organomet. Chem.* 34 (2020) e6016.
- B. Gültekin, D. İ. Özbağcı, İ. Aydın, R. Aydın, F. Arı, Y. Zorlu, New copper(II) complexes containing tryptophan based Schiff bases as promising antiproliferative agents on breast cancer cells, *J. Mol. Struct.*, 1301 (2024) 137273.
- D.İ. Özbağcı, B. Gültekin, İ. Aydın, R. Aydın, F. Arı, Y. Zorlu, New copper (II) complexes bearing tryptophan-based Schiff bases and 2,2'-bipyridine: Crystal structures, DNA/BSA interactions and antiproliferative activities, *Appl. Organomet. Chem.*, 38(4) (2024) e7369.
- J.R. Lakowicz, G. Weber, Quenching of fluorescence by oxygen. A probe for structural fluctuations in macromolecules, *Biochemistry*, 12 (21) (1973) 4161-4170.
- K.D. Karlin, B.I. Cohen, J.C. Hayes, A. Farooq, J. Zubieta, Models for methemocyanin derivatives: structural and spectroscopic comparisons of related azido-coordinated (N₃⁻) mono- and dinuclear copper(II) complexes, *Inorg. Chem.* 26 (1) (1987) 147-153.

20. M. Lee, A. L. Rhodes, M.D. Wyatt, S. Forrow, J.A. Hartley, GC base sequence recognition by oligo(imidazolecarboxamide) and C-terminus-modified analogues of distamycin deduced from circular dichroism, proton nuclear magnetic resonance, and methidium propylethylenediaminetetraacetate-iron(II) footprinting studies, *Biochemistry*, 32 (16) (1993) 4237-4245.
21. L.N. Zhang, F.Y. Wu, A.H. Liu, Study of the interaction between 2,5-di-[2-(4-hydroxy-phenyl)ethylene]-terephthalonitril and bovine serum albumin by fluorescence spectroscopy. *Spectrochim. Acta A Mol. Biomol. Spectrosc.*, 79 (2011) 97-103.
22. X.X. Cheng, Y. Lui, B. Zhou, X.H. Xiao, Y. Liu, Probing the binding sites and the effect of berbamine on the structure of bovine serum albumin, *Spectrochim. Acta Part A Mol. Biomol. Spectrosc.*, 72 (2009) 922-928.
23. S. Prasanth, D.R. Raj, T.V. Vineeshkumar, R.K. Thomas, C. Sudarsanakumar, Exploring the interaction of L-cysteine capped CuS nanoparticles with bovine serum albumin (BSA): a spectroscopic study, *RSC Adv.*, 6 (2016) 58288-28295.
24. T. Göktürk, T. Zengin, T. Hökelek, C.G. Topkaya, R. Güp, Synthesis, Crystal Structure, Hirshfeld Surface Analysis, DNA/BSA Interaction and Molecular Docking Studies of 2-(6-(4-chlorophenyl)-1,2,4-triazin-3-yl)quinoline, *J. Mol. Struct.*, 1292 (2023) 136128.
25. K. Preetha, E. Seena, P.K. Maniyampara, E. Manoj, M.P. Kurup, Synthesis, crystal structure, Hirshfeld surface analysis, DFT, molecular docking and in vitro antitumor studies of (2E)-2-[4-(diethylamino)benzylidene]-N-ethylhydrazinecarbothioamide, *J. Mol. Struct.*, 1295 (2024) 136700.
26. S.K. Tarai, S. Mandal, A. Tarai, I. Som, A. Pan, A. Bagchi, A. Biswas, S.C. Moi, Biophysical study on DNA and BSA binding activity of Cu(II) complex: Synthesis, molecular docking, cytotoxic activity, and theoretical approach, *Appl. Organomet. Chem.*, 37(8) (2023) e7164.
27. S.K. Tarai, A. Tarai, S. Mandal, B. Nath, I. Som, R. Bhaduri, A. Bagchi, S. Sarkar, A. Biswas, S. Ch. Moi, Cytotoxic behavior and DNA/BSA binding activity of thiosemicarbazone based Ni(II) complex: bio-physical, molecular docking and DFT study, *J. Mol. Liq.*, 383 (2023) 121921.
28. T. Tantimongcolwat, S. Prachayasittikul, V. Prachayasittikul, Unravelling the interaction mechanism between cloquinol and bovine serum albumin by multi-spectroscopic and molecular docking approaches, *Spectrochim. Acta Part A Mol. Biomol. Spectrosc.*, 216 (2019) 25-34.
29. T. Kroetz, P.A. Nogara, F. da Silveira Santos, L.C. da Luz, V. S. Câmara, J.B.T. da Rocha, A. Gonçalves Dal-Bó, F. S. Rodembusch, Interaction Study between ESIPT Fluorescent Lipophile-Based Benzazoles and BSA, *Molecules*, 26(21) (2021) 6728.
30. W. Widowati, A.P. Rani, R.A. Hamzah, S. Arumwardana, E. Afifah, H. S.W. Kusuma, D.D. Rihibiha, H. Nufus, A. Amalia, Antioxidant and Antiaging Assays of Hibiscus sabdariffa Extract and Its Compounds, *Nat. Prod. Sci.*, 23(3) (2017) 192-200.